

SLS-TME-TA-2005-0278
9th September 2005

Experimental Determination of the Point-Spread Function for the Optical Diagnostics Setup at the 100 keV Gun Test Stand

Åke Andersson, Simon C. Leemann

Paul Scherrer Institut, CH-5232 Villigen PSI, Switzerland

Abstract

In the scope of the LEG Project [1] a 100 keV gun test stand is currently being built [2]. The test stand will contain various diagnostic equipment [3] in order to characterize the 100 keV electron beam. One of the most important parameters to be measured is the beam emittance which requires obstruction of a major part of the beam with different kinds of slit/pinhole arrays. The part of the beam passing the obstruction, the so-called 'beamlets', will hit a phosphor screen downstream. The light pattern produced in the phosphor will then be used to reconstruct the horizontal and vertical phase space of the electron beam. In order to properly measure the light pattern we are relying on a commercial zoom optic system (Thales Optem Telecentric Zoom 100) and CCD camera (Sony XC-55) together with an in-house frame-grabber system used widely at SLS. The aim of the experiments reported in this note is to investigate how well a measured image corresponds to the real light pattern. For this the so called Point-Spread Function (PSF) is experimentally determined.

1 Introduction

The experimental setup is schematically shown in figure 1. The goal is to determine the Point-Spread Function (PSF) for the zoom optics, the CCD camera and the frame-grabber system *as a unit*. Usually, the Point-Spread Function for an optical system is defined as the two-dimensional intensity distribution in the image plane, produced by a point source in the source plane. In our notation, the Point-Spread Function is the two-dimensional *measured* light distribution, produced by a point source. Therefore, we include all possible diluting contributions, not only optical aberrations and diffraction effects, but also for example CCD readout noise, CCD pixel resolution, frame grabber ADC noise, vibrations etc. While measuring the PSF we also tried to optimize the whole setup, which is then equivalent to minimizing the PSF. This includes for example to adjust carefully the CCD chip plane correctly to the image plane. Finally, all different adjustments then gave good "hands-on feeling" for what are the most delicate issues to consider in order to reach optimal results.

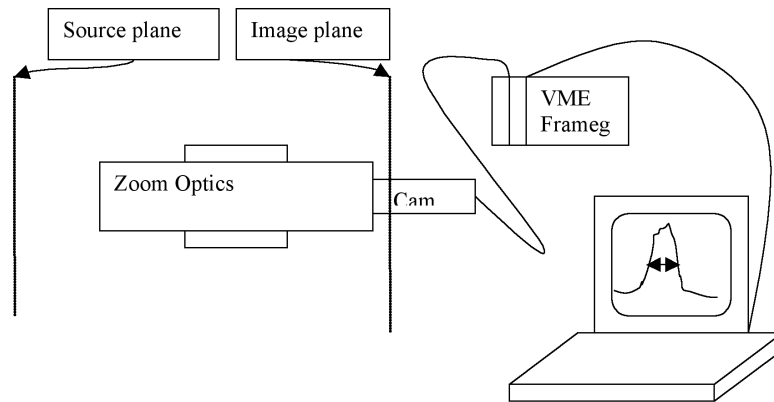


Figure 1: Schematic of the experimental setup.

2 Measurements

We started the measurement series by using a pinhole array. Each pinhole is $15\ \mu\text{m}$ in diameter; the horizontal and vertical distances between the pinholes is $0.7\ \text{mm}$ and $0.4\ \text{mm}$ respectively. The precision of these measures is still not quite clear, but roughly the accuracy should be 1% for the spacing and 5–10% for the actual diameter. The thickness of the pinhole array plate is $150\ \mu\text{m}$. This thickness is small enough not to cause any ambiguity problems defining the source plane. The source is arranged as depicted in figure 2. A halogen lamp is pointed towards a diffuser, which in turn illuminated the pinholes. In this way the pinholes should be uniformly illuminated and the light emerging from each part of the pinhole should be uniform in intensity over the entire area of the pinhole. Only the pinholes close to the optical axis are used for calibration and PSF measurements; we postpone the study of the PSF for point sources far away from the optical axis.

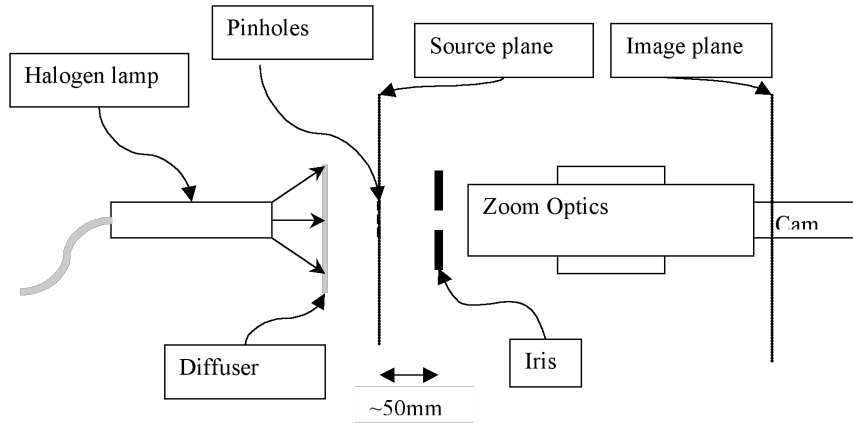


Figure 2: Schematic of the source and optics setup.

All measurements were performed at the maximum zooming of the zoom optics. With this setting the calibration factor was $(3.81 \pm 0.05)\ \mu\text{m}/\text{pixel}$ in both directions. If always the same four pinholes were used, the uncertainty decreased to $\pm 0.01\ \mu\text{m}/\text{pixel}$, but the measured value then depended on the quartet chosen. This gave the indication that the measuring system was more accurate than the mechanical distances between the holes. According to the vendor, the CCD camera has a pixel size (center to center) of $7.4\ \mu\text{m}$ in both directions. These numbers give magnification factors of 1.94 in both directions in good agreement with manufacturer specifications stating a magnification of 1.9 [4]. Figures 3–6 show horizontal and vertical profiles for one pixel row respectively column, going through the most intense pixel. All profiles are scaled up to roughly 255 units (8 bit ADC) at the peak. Therefore, in order to judge the true peak intensity in the 0 to 255 unit scale, is to observe the background level. Figure 3 shows an

image taken with a maximum very close to 255 units (increased halogen lamp setting) and a background around 16 units. Figure 4 shows profiles for a lower peak intensity (decreased halogen lamp setting), resulting in a higher background level of approximately 25 units. This corresponds to a peak intensity of roughly $16/25 \times 255 = 163$ units. The RMS values of the Gaussian fits are almost identical for the two samples, indicating that the linearity of the CCD is good enough in this intensity interval. We believe that the linearity is good in a much wider intensity range, but since it is not specified in the camera manual, we chose to at least verify it in the region of interest. Going to peak intensity values lower than 100 is not preferable due to poorer fit accuracy.

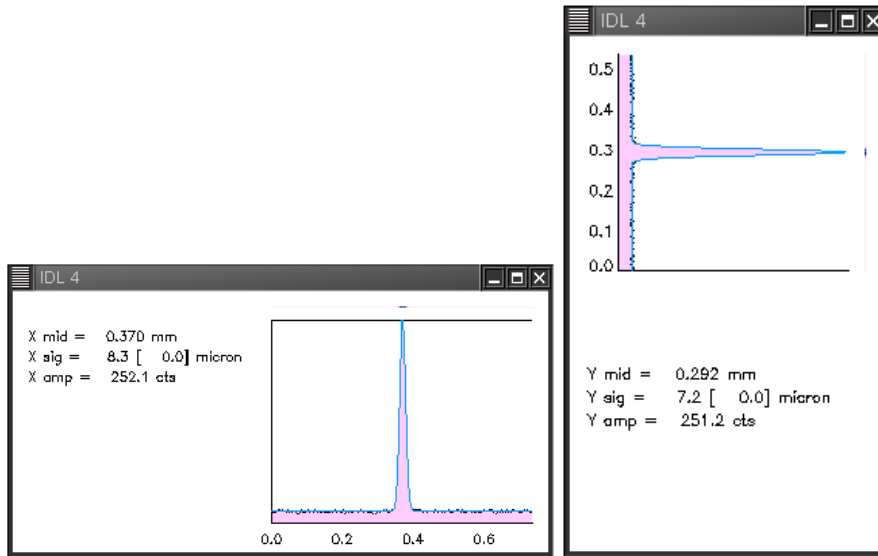


Figure 3: Horizontal and vertical profiles for a $15 \mu\text{m}$ pinhole with halogen lamp set to high intensity and iris set to accept ≈ 45 mrad.

Figure 3 shows an optimized iris setting; pixel amplitude was maximized (without getting into saturation) while maintaining the smallest spot size. For this optimum, we set the iris opening in front of the zooming optics to accept a circular opening angle of ≈ 45 mrad ($= r_{iris}/l_{source-iris}$). Figures 5 and 6 show the resulting profiles when the opening angle is ≈ 65 mrad and ≈ 25 mrad respectively. For 65 mrad opening angle there are clear tails in the image profiles. We believe that the zoom optics do not handle the peripheral light as well as the close-to-axis light. It seems to have internal irises limiting the acceptance angle between 60 and 65 mrad, but one gains in image quality by going down to at least 55 mrad. This confirms the specifications given by the manufacturer stating that the numerical aperture is 0.062 at magnification 1.9 [4]. In the interval between 55 and 35 mrad the image quality stays almost constant, while going further down to 25 mrad the diffraction effect starts to dominate, as can be seen in Figure 6.

Figure 7 shows the horizontal and vertical profiles for a $10 \mu\text{m}$ pinhole, using a

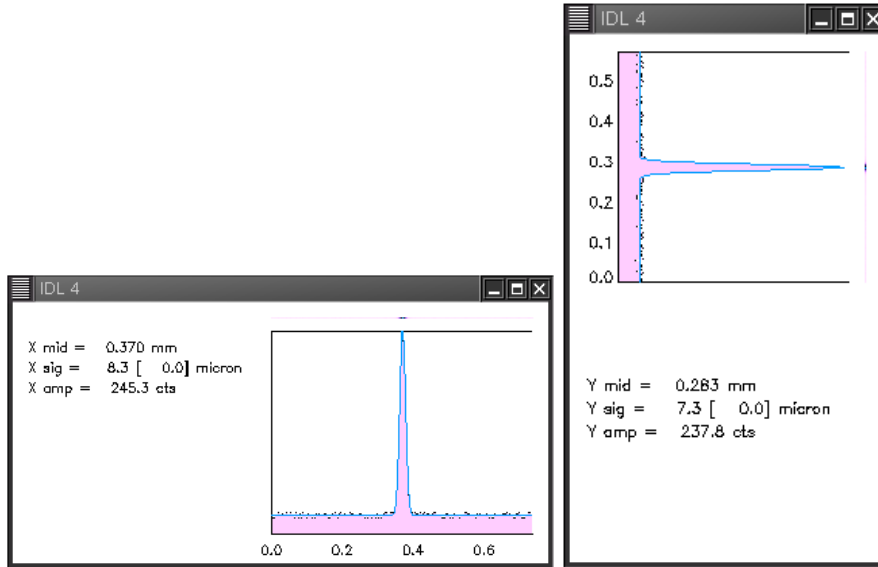


Figure 4: Horizontal and vertical profiles for a 15 μm pinhole with halogen lamp set to reduced intensity and iris set to accept ≈ 45 mrad.

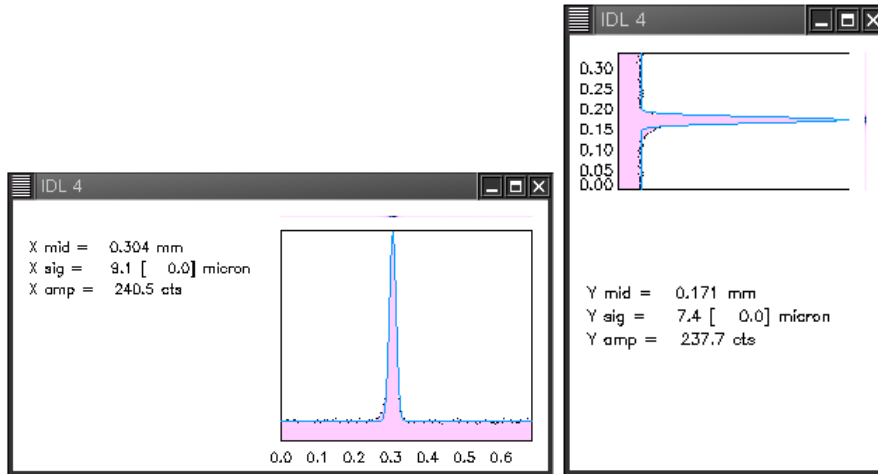


Figure 5: Horizontal and vertical profiles for a 15 μm pinhole with halogen lamp set to reduced intensity and iris fully open accepting ≈ 65 mrad. Tails presumably due to off-axis light are clearly visible.

limiting aperture to block off-axis rays. The sigma values should be multiplied by the calibration factor 3.81, resulting in $\sigma_x = 5.7 \mu\text{m}$ and $\sigma_y = 5.3 \mu\text{m}$. For comparison, figure 8 shows the profiles without blocking the off-axis rays. Figure 9 shows the horizontal and vertical profiles for a 5 μm pinhole, using a limiting aperture to block off-axis rays. Again, the sigma values should be multiplied by 3.81, resulting in $\sigma_x = 3.8 \mu\text{m}$ and $\sigma_y = 3.4 \mu\text{m}$. For comparison, figure 10 shows the profiles without blocking the off-axis rays.

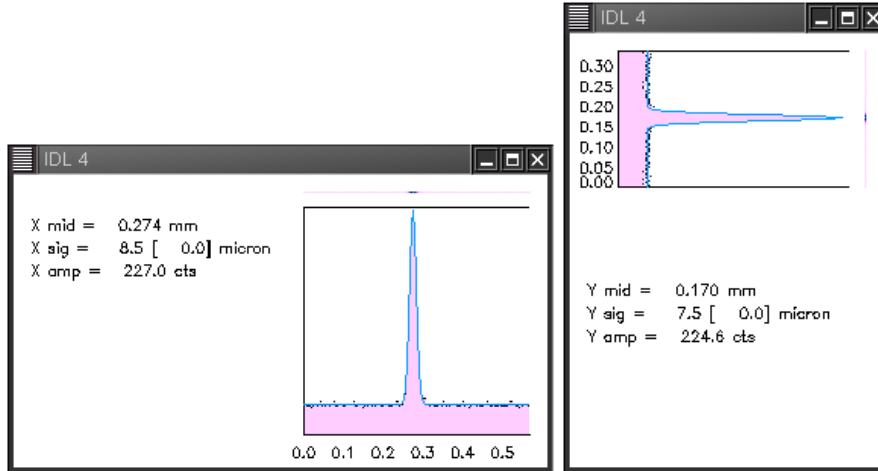


Figure 6: Horizontal and vertical profiles for a 15 μm pinhole with halogen lamp set to high intensity and iris closed accepting ≈ 25 mrad.

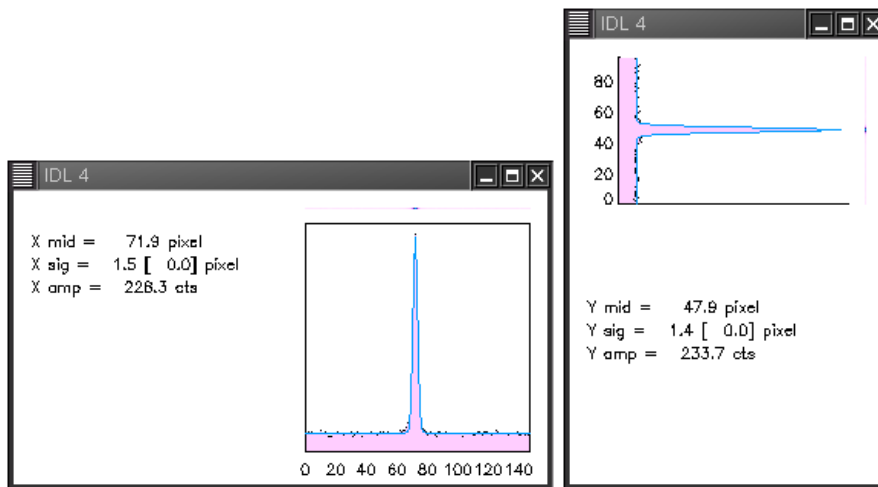


Figure 7: Horizontal and vertical profiles for a 10 μm pinhole with halogen lamp set to reduced intensity and iris set to accept ≈ 45 mrad. The $\sigma_{x,y}$ have to multiplied by the calibration factor 3.81, resulting in $\sigma_x = 5.7$ μm and $\sigma_y = 5.3$ μm .

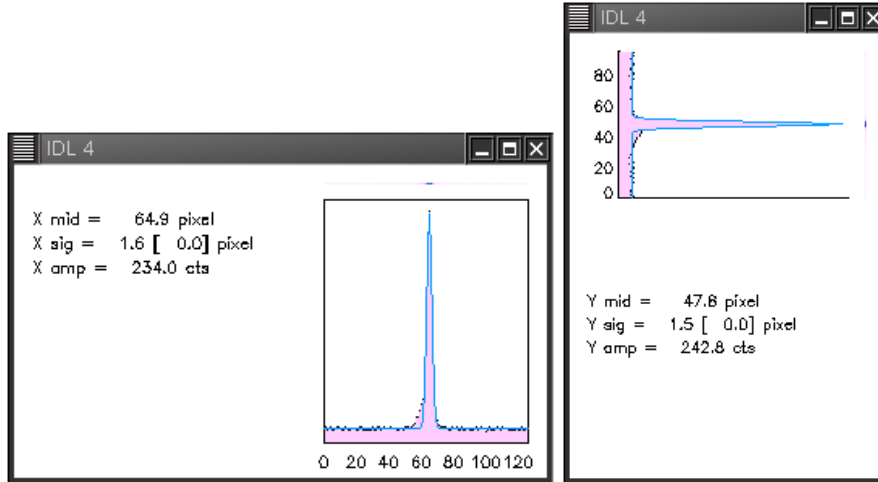


Figure 8: Horizontal and vertical profiles for a $10 \mu\text{m}$ pinhole with halogen lamp set to reduced intensity and iris fully open accepting $\approx 65 \text{ mrad}$. The $\sigma_{x,y}$ have to multiplied by the calibration factor 3.81, resulting in $\sigma_x = 6.1 \mu\text{m}$ and $\sigma_y = 5.7 \mu\text{m}$. Tails presumably due to off-axis light are clearly visible.

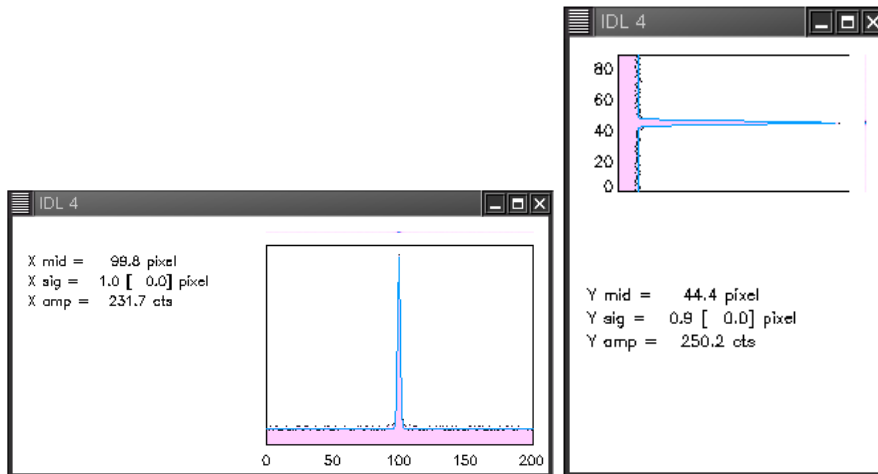


Figure 9: Horizontal and vertical profiles for a $5 \mu\text{m}$ pinhole with halogen lamp set to high intensity and iris set to accept $\approx 45 \text{ mrad}$. The $\sigma_{x,y}$ have to multiplied by the calibration factor 3.81, resulting in $\sigma_x = 3.8 \mu\text{m}$ and $\sigma_y = 3.4 \mu\text{m}$.

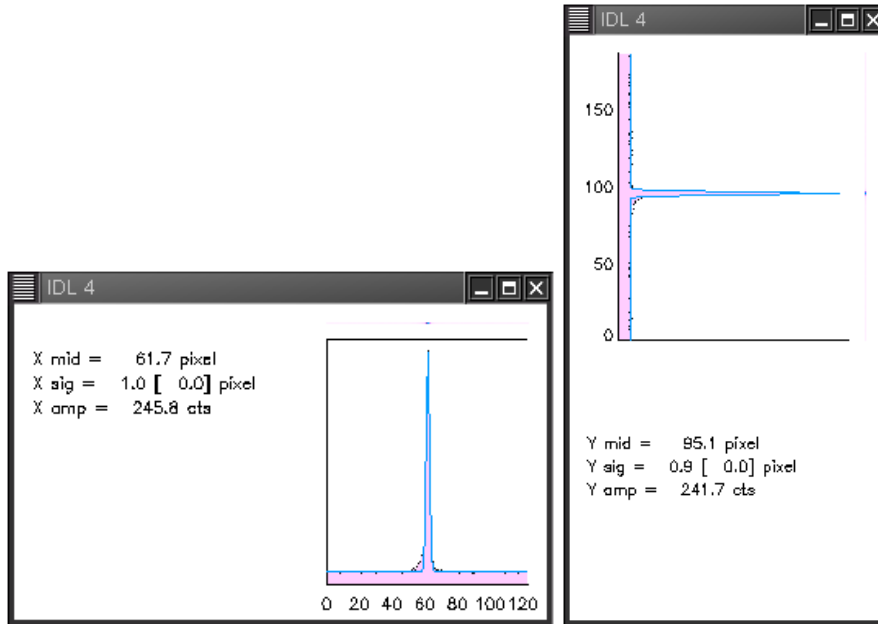


Figure 10: Horizontal and vertical profiles for a $5 \mu\text{m}$ pinhole with halogen lamp set to high intensity and iris fully open accepting $\approx 65 \text{ mrad}$. The $\sigma_{x,y}$ have to be multiplied by the calibration factor 3.81, resulting in $\sigma_x = 3.8 \mu\text{m}$ and $\sigma_y = 3.4 \mu\text{m}$. Tails presumably due to off-axis light are clearly visible.

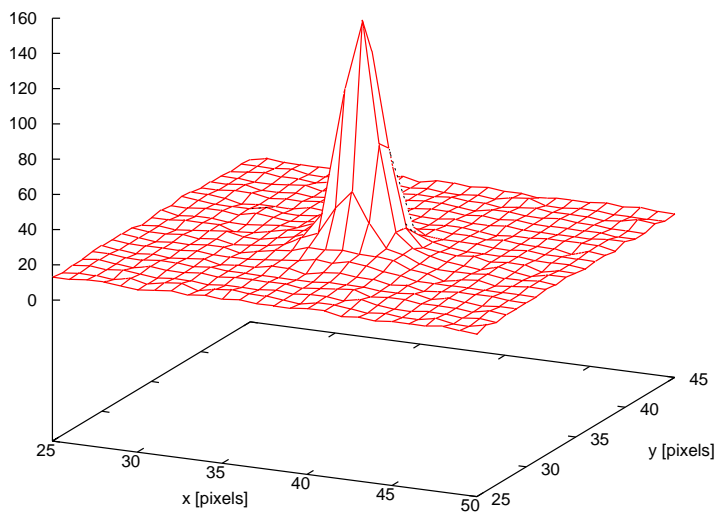


Figure 11: Two-dimensional intensity plot of a $5 \mu\text{m}$ pinhole with halogen lamp set to high intensity and iris set to accept $\approx 45 \text{ mrad}$. The results of the Gaussian fits for the entire hole image are $\sigma_x = 4.2 \mu\text{m}$ and $\sigma_y = 3.8 \mu\text{m}$.

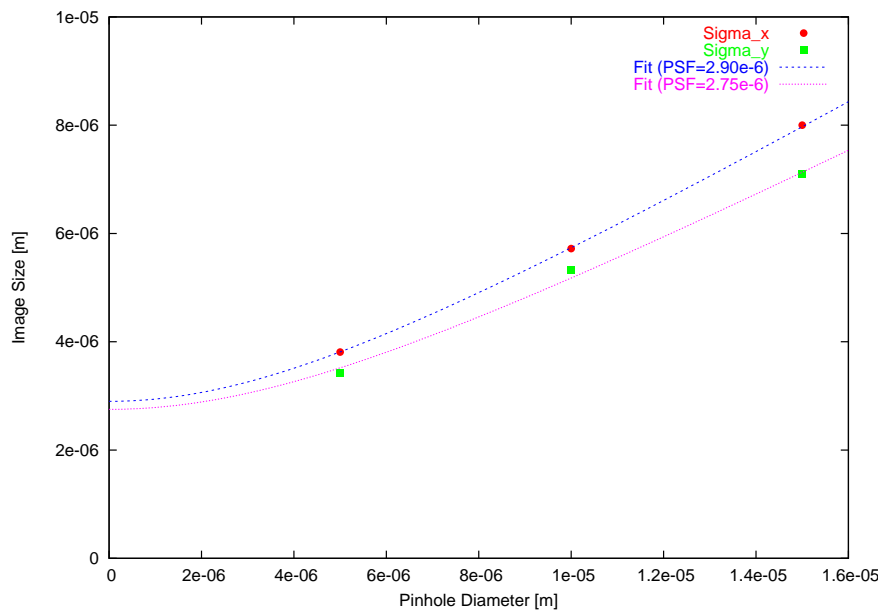


Figure 12: Measured image size vs. pinhole diameter. A rough fit is indicated giving a PSF of $2.9 \mu\text{m}$ respectively $2.75 \mu\text{m}$; both fit results have $\approx 10\%$ error.

3 Discussion

The measurements were performed in order to determine the point-spread function of the system. Judging by figure 12, the system seems to have the potential of a point-spread function with a RMS certainly lower than 3.4–3.8 μm , since the dependence on pinhole size still behaves quite linear all the way down to 5 μm pinhole diameter. The fit on this data indicates a PSF slightly below 3 μm , but for the moment we can only state with certainty that the PSF RMS value is less than 3.4–3.8 μm . In a future measurement one would of course use a pinhole with considerably smaller diameter to see the actual PSF. Further one should think of using a bandpass filter around 540 nm, in front of the pinhole. This is because the phosphor being installed at the gun test stand is P43, which emits roughly 80% in a quite narrow band (12 nm FWHM) around 540 nm. We expect the problem there will be to get enough light intensity through both a smaller pinhole and narrower bandwidth.

On the other hand one cannot expect a strong decrease in the PSF, since the diffraction pattern (Airy pattern) alone will give a limit 2.9 μm at 540 nm and 42 mrad opening angle.

In order to better resemble the actual measurement conditions at the gun test stand, one should additionally install an identical quartz vacuum window right after the pinhole for future measurements of the PSF.

Another issue for further investigations is the strange behavior consistently giving a smaller result in the vertical direction than in the horizontal. During the period of measurements we tried to exclude the possibility of a CCD deficiency (by turning the camera 90 degrees) and the possibility of a pinhole deficiency (by turning the pinhole 90 degrees). The results were still the same, and the question remains open.

References

- [1] The Low Emittance Gun Project LEG at PSI, <http://leg.web.psi.ch>
- [2] S. C. Leemann, *100 keV Gun Test Stand: Design and Parameter Study*, SLS Internal Note, SLS-TME-TA-2004-0244, 2004, <http://slsbd.psi.ch/pub/>
- [3] S. C. Leemann, V. Schlott, A. Streun, *Design of the 100 keV DC Gun Test Stand*, PSI Scientific and Technical Report 2004, Volume VI, 2004, <http://leg.web.psi.ch/public/publications/Leemann-yr04.pdf>
- [4] Thales Optem, Telecentric Zoom 100, <http://www.thales-optem.de>